

Enhancing the Latent Fingerprint Segmentation Accuracy Using Hybrid Techniques – WCO and BiLSTM

Neha Chaudhary¹, Priti Dimri²

¹Research Scholar-Uttarakhand Technical University, Department of computer science and engineering, Dehradun, Uttarakhand, India

²Professor, Department of computer science and Application, G B Pant Engineering College, Gaurdauri, Uttarakhand, India

¹nehacisco15@gmail.com, ²pdimri1@gmail.com

Abstract - For more than a century, latent fingerprints have been effectively utilized to identify criminal defendants by matching the latent fingerprints to the rolled or plain fingerprints saved in the dataset. Background noise, overlapping patterns, unclear structures, partial impressions, and non-linear distortions of the finger are the key issues with latent fingerprints. Segmentation is one of the procedures that must be completed before identification. Traditional segmentation methods perform badly on latent fingerprints. The focus of this research has primarily been on the automatic segmentation of latent fingerprints. First, the latent fingerprint images are divided into local blocks. Then, feature vectors are constructed by extracting the features from the local blocks using the ridge, intensity, and gradient method. Extracted feature vectors are fed as input of bidirectional long short-term memory network (BiLSTM). The BiLSTM is utilized for segmentation with world cup optimization for weight update. The proposed algorithm's performance is compared with the previously known results of the latent fingerprint segmentation techniques. The segmentation accuracy of latent fingerprints is 92.9% which has greatly been improved, and it is quite promising than the earlier algorithms.

Keywords - Segmentation, latent fingerprint, ridge features, bidirectional long short-term memory network.

I. INTRODUCTION

Fingerprints are used to identify criminals by comparing the similarity between the latent fingerprints with the referenced database. Latent fingerprints are not visible by a naked eye due to the poor quality unless some chemical and physical methods are applied to enhance them [1]. To identify the terrorists and criminals, latent fingerprints are the main evidence for law enforcement agencies [2]. Factors such as uneven contrast, low visibility, unclear ridge structure, and overlapped print make the quality of the latent fingerprints very poor [3].

The latent fingerprint examiner manually detects the features of latent fingerprints due to their poor quality so that an automated fingerprint identification system can match them against the referenced database (AFIS). The

success of AFIS is dependent on segmentation, which is the primary stage in the system. There are three sorts of fingerprint images: (1) plain fingerprints, (2) rolled fingerprints, and (3) latent fingerprints.



Fig. 1 depicts many fingerprint image classes. (1) Plain fingerprint, (2) Rolled fingerprint, and (3) Latent fingerprint (IIT-D).

Plain fingerprints are obtained by placing the fingers on a flat surface. Rolling fingerprints are those obtained by rolling the fingers across the surface from one side to the other. Plain and rolled fingerprints are of good quality and include enough information to be matched with the database. Latent fingerprints are accidentally left by offenders at crime scenes and are frequently combined with other components such as other fingerprints or structure noise.

Segmentation is the process that segregates the foreground and the background. The foreground contains the region of interest, also called fingerprint area, and the background contains the noisy area. To extract the features of fingerprints which is a singular point and minutiae, exact segmentation must be extracted. Minutiae and singular points are the key features of the fingerprint matching process. When algorithms of features extraction method are applied directly on the fingerprint image without segmentation, it gives more false features and increases the matching error. The main aim of the fingerprint segmentation algorithm is to find the fingerprint area, discard the noisy area, increase the matching accuracy and reduce the extraction of false features.



II. LITERATURE SURVEY

Many algorithms have been developed for fingerprint segmentation. In the previous work [4], segmentation is achieved by directional images. In this research paper, the image is divided into several blocks then blocks are classified into foreground and background based on the variance information. The segmentation method used by Mehtre et al. [4] was further enhanced [5], which combines the directional and variance information of fingerprint image segmentation. Blocks are classified according to the grayscale variance along a scanline perpendicular to the orientation of ridge flow [6]. Fingerprints are segmented based on mean, variance, and coherence information [7]. Xue and Li [8] proposed a segmentation technique based on orientation field estimation and statistical characteristics of gray, which combines the statistical characteristics of gray (mean and variance) with orientation information (point and block information) for fingerprint image segmentation.

These Algorithms [4-8] provide good segmentation results on fingerprints, but latent fingerprint segmentation remains a challenge.

Several algorithms [9-12] have already been developed for latent fingerprint segmentation. Zhang et al. [9] proposed a total variation model for latent fingerprint segmentation. The total variation model includes a fidelity weight coefficient that automatically adjusts according to the image content and adaptively adjusts the background noise level. The adaptive Total Variation (ATV) model provides high accuracy for good latent fingerprints but low accuracy for noisy ones. Lai et al. [10] proposed a Total Directional Variation (DTV) approach integrating spatial - texture orientations in total variation computation. DTV model provides a better computation outcome as compared to the total variance L1 fidelity model. Zhang et al. [11] further extended these models to the Adaptive Directional Total Variation (ADTV) model, which uses the success framework of both ATV and DTV for latent fingerprint segmentation. Choi et al. [12] used two features to segment latent fingerprints: frequency and ridge. In this method, the fingerprint area is identified separately by the frequency, ridge features, and the intersection of both regions is used to determine the final segmented region. Short et al. [13] presented a ridge template correlation approach for the latent fingerprint segmentation model, reducing the fingerprint area from 60.7 percent to 33.6 percent while increasing the real minutiae rate in the fingerprint region. In a different test, true minutiae counted as background reduced from 1.41% to 0.29%. In 2014, Cao et al. [14] proposed a new method of latent fingerprint segmentation and the enhancement that is based on the coarse and fine ridge structure dictionary, and this model separates the fingerprint image into local blocks and segments the latent fingerprint based on a local block's resemblance to an ideal ridge pattern template. NSIT SD-27 and WVU DB are two databases used for latent fingerprint segmentation. Rank-1, 70.16% identification was reported on the WVU database and 61.24% on NSIT SD-27.

Sankaran et al. [15] developed a feature extraction and random decision forest classification model for latent fingerprint segmentation that utilizes five distinct feature categories integrated for latent fingerprint segmentation. The efficiency of the proposed algorithm was measured based on SIVV-TPR, rank-k identification, and segmentation accuracy. Chaudhary, N [30], Define the neural network model for latent fingerprint Segmentation. Stojanović [16] proposed an overlapped fingerprint segmentation algorithm based on CNNs, and this model divides the fingerprint region into single, overlapped, and background classes. These algorithms are compared in [27].

III. STRUCTURED NOISES

Latent fingerprint segmentation poses two challenges primarily. First, the latent fingerprints have low visibility, poor quality, and distorted ridge, which results in the latent fingerprint containing only 15 minutiae whereas the rolled fingerprint contains 80 minutiae [17] and second, various types of structured noises are found in latent fingerprints; these structured noises (seen in figure 2) are divided into six categories: line, stain, arch, character, speckle, and others.

Line-The line noise can be presented in the form of multiple parallel or single lines. Removing the multiple parallel lines from the fingerprint is a typical task because they share some common features. Hough transformation-based methods can be used to remove the single line from the fingerprint.

Stain- Strain noise is generated when a fingerprint is put on a dirty or wet surface. The brightness of strain becomes heterogeneous and its sponge in shape.

Arch- When investigators manually label the region of interest in a crime scene, arch noise is produced.

Character- Character noise can be typed or written by hand. It can be presented in a variety of sizes, shapes, and brightness.

Speckle-It contains a tiny structure like dots, dust speckles.

Others-It includes other types of noise like the sign, arrow, etc. This type of noise contains sharp edges with smooth surfaces.

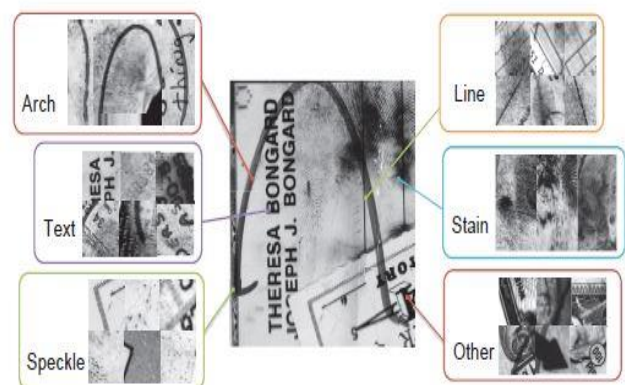


Fig. 2 Different Types of Structured Noise Present in Latent Fingerprint [11].

Such noises may be present in the fingerprint. The primary purpose of segmentation is to isolate the noise from the fingerprint region. In the proposed work, a new algorithm for the automatic segmentation of latent fingerprints has been introduced.

IV. PROPOSED METHODOLOGY

The methodology of the proposed work is shown in Fig. 3. The proposed fingerprint segmentation technique uses a two-way approach to extract fingerprint area from the latent fingerprint. The latent fingerprint image is first broken into $b*b$ size blocks, and then features of the local block are retrieved using the gradient, intensity, and ridge approach. The outputs of the feature extraction method are feature vectors. These feature vectors are fed as an input of the BiLSTM, the WCO algorithm is used for weight update in BiLSTM. WCO algorithm for the weight update has been used because it provides the global-optimal solution.

This section introduces a proposed segmentation technique and describes how it can be used to separate the foreground and background of the fingerprint successfully. It combines the feature extraction approach and BiLSTM with WCO. The block-wise segmentation technique for latent fingerprints is depicted in Fig. 3.

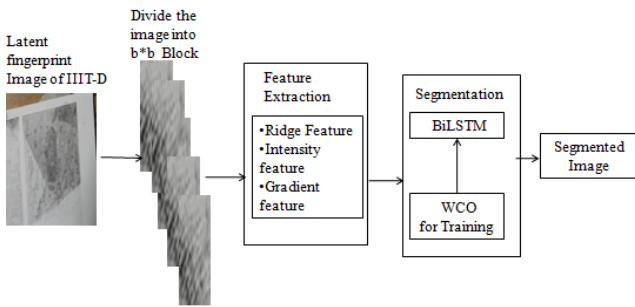


Fig. 3 Workflow of proposed work

A. Feature Extraction Method

To determine whether the $b*b$ patch belongs to the fingerprint image, the pattern has to be extracted specific to the fingerprint (e.g., Ridge pattern). Earlier, many proposed algorithms defined the ridge pattern for live scan and inked fingerprints [18, 19, 20, and 21]. In this research, intensity, ridge, and gradient features have been employed, which are used to differentiate the foreground and background image.

a) Intensity-based features

In an intensity-based feature, patches can be classified as fingerprint or non-fingerprint based on their intensity value because the intensity value of the foreground differs from the background. The intensity values can be estimated as follows:

1) Variance

The variance of the fingerprint patches is high as compared to the non-fingerprint patches. The variance of the $b*b$ size patch can be calculated as follow:

$$f1 = \frac{1}{b^2} \sum_{x=1}^b \sum_{y=1}^b \left(I(x, y) - \frac{1}{b^2} \sum_{x=1}^b \sum_{y=1}^b I(x, y) \right)^2 \quad (1)$$

2) Differences of mean

It calculates the difference between the mean of local and global intensity. As a result, the mean difference should ideally be greater in the background than in the foreground. The mean difference can be calculated as follows:

$$f2 = \left(\frac{1}{b^2} \sum_{x=1}^b \sum_{y=1}^b I(p, q) \right) - I_{mean} \quad (2)$$

I_{mean} represents the complete image intensity.

3) Ridge Cluster value

The different features of Mean and Variance are combined in ridge cluster value to show the fingerprint structure (Ridge and Valley) in the foreground region. It can be calculated as [22]:

$$f3 = \sum_{x=1}^b \sum_{y=1}^b z1(x, y) \times z2(x, y) \quad (3)$$

Where,

$$z1(x, y) = \begin{cases} 1 & \text{if } I(x, y) < I_{mean} \\ 0 & \text{otherwise} \end{cases} \quad (4)$$

$$z2(p, q) = \begin{cases} 1 & \text{if } t(x, y) < \left(\frac{b^2}{2} + 1 \right) \\ 0 & \text{otherwise.} \end{cases} \quad (5)$$

$$t(x, y) = \sum_{i=x-\frac{b}{2}}^{x+\frac{b}{2}} \sum_{j=y-\frac{b}{2}}^{y+\frac{b}{2}} z1(i, j) \quad (6)$$

Where t is the number of pixels and I_{mean} is the global mean intensity in the neighborhood, $b*b$ size patch with intensity lower than I_{mean} is measured. The number of pixels of each block whose t value is less than the specific threshold value is calculated by $f3$.

b) Ridge Based Feature

These types of features are very useful to identify the actual fingerprints from latent fingerprints. Four different features based on the ridge can be calculated as follow:

1) Average inter-ridge distance

The fingerprint area has a greater amount of ridges. The inter-ridge distance in the non-fingerprint area would be greater than in the fingerprint area [19]. The average inter-ridge distance is computed as follows:

$$f4 = \frac{\sum_{e=1}^N E_e}{Q-1} \quad (7)$$

Where Q is the count of ridge peaks, and E_e is the distance between two consecutive peak values.

2) Ridge Frequency

Fourier transform [23] is applied to calculate ridge frequency to each $b*b$ patch. It can be calculated as:

$$f5 = \text{argmax} \left(\sum_{x=1}^b \sum_{y=1}^b |D(x, y)| * T_a(x, y) \right) \quad (8)$$

Where $T_a(x, y)$ is the a^{th} directional filter and $D(x, y)$ is the output of the Fourier transform of $b*b$ patch. Ridge frequency of patch is the frequency at which filter gives the maximum response.

3) Peak height variance in ridges

The ridge pressure variation in the b*b patch can be estimated as follows:

$$f6 = \frac{\sum_{a=1}^N (Q_i - Q_{mean})}{0-1} \quad (9)$$

Peak ridge height value is Q for ath ridge, N is the number of the ridge in the peak, and peak ridge height across all patches is Q_{mean}. A low response means a non-fingerprint region rather than a fingerprint region.

4) Ridge energy

This feature provides the “ridgeness” of the patch. The “ridgeness” of the patch is very useful for the segmentation of latent fingerprints. This feature can be calculated as follows [24]:

$$f7 = \frac{1}{b^2} \left(\sum_{x=1}^b \sum_{y=1}^b (|D(x,y)| * T_a(x,y))^2 \right) \quad (10)$$

Where ath directional filter denoted by T_a(x, y).

c) Gradient-based features

The gradient measures the directional change in pixel intensity. The gradient can be used to estimate orientation. Orientation at location (x, y) can be computed as:

$$O(x,y) = \begin{cases} \pi/4, & g = 0, h < 0 \\ 3\pi/4, & g = 0, h \geq 0 \\ \theta(x,y) + \pi/2, & g > 0 \\ \theta(x,y), & g < 0, h \leq 0 \\ \theta(x,y) + \pi, & g < 0, h > 0 \end{cases} \quad (11)$$

Where θ(x, y) can be calculated as:

$$\theta(x,y) = \frac{1}{2} \tan^{-1} \left(\frac{h}{g} \right) \quad (12)$$

$$g = \sum_{x=1}^b \sum_{y=1}^b (I_h^2(x,y) - I_v^2(x,y)) \quad (13)$$

$$h = \sum_{x=1}^b \sum_{y=1}^b 2 * I_h(x,y) * I_v(x,y) \quad (14)$$

I_h and I_v are the gradients along with h and v direction, The gradient-based feature can be calculated as follows:

1) Squared gradient sum

Interleaving valley and ridge patterns are maximum for a fingerprint as compared to the non-fingerprint. The Interleaving valley and ridge pattern can be calculated as:

$$f8 = \sqrt{g^2 + h^2} \quad (15)$$

2) Orientation of the ridge

Gaussian smoothing kernel is used for smoothing the orientation of patches [23],

$$f9 = \frac{1}{b^2} \sum_{x=1}^b \sum_{y=1}^b RO'(x,y) \quad (16)$$

$$RO'(x,y) = \frac{1}{2} \tan^{-1} \left(\frac{\sin(2RO(x,y))*G(x,y)}{\cos(2RO(x,y))*G(x,y)} \right) \quad (17)$$

Gaussian smoothing kernel and orientation RO(x, y) is defined in equation 11. The sum of the norm of the squared gradient vector is calculated as follows:

$$f10 = \sum_{x=1}^b \sum_{y=1}^b (I_h^2(x,y) - I_v^2(x,y))^2 + (2 * I_h(x,y) * I_v(x,y))^2 \quad (18)$$

Thus, all 10 features (f1, f2.....f10) are used to separate the fingerprint region from the non-fingerprint region. All features form a matrix of vectors. This vector matrix is the input of the next phase.

B. Segmentation

Segmentation aims to separate the foreground and background in the latent fingerprint. For the segmentation of the latent fingerprint, the BiLSTM model is used. The Input of the BiLSTM [25] is the output of the feature extraction module in the form of a matrix. The WCO algorithm is also used for weight update in BiLSTM [26] to reduce the gradient vanishing problem.

a) The bidirectional long-short term memory

LSTM networks (units) are discrete architectures that comprise memory cells, memory blocks, and gate units. LSTM employs three gates: an input gate, an output gate, and a forget gate. The input gate controls the memory cell's input, the output gate controls the memory cell's output to the other LSTM block, and the forget gate in the memory block structure is controlled by a basic one-layer neural network. The internal structure of the LSTM [31] memory block is depicted in Fig. 4.

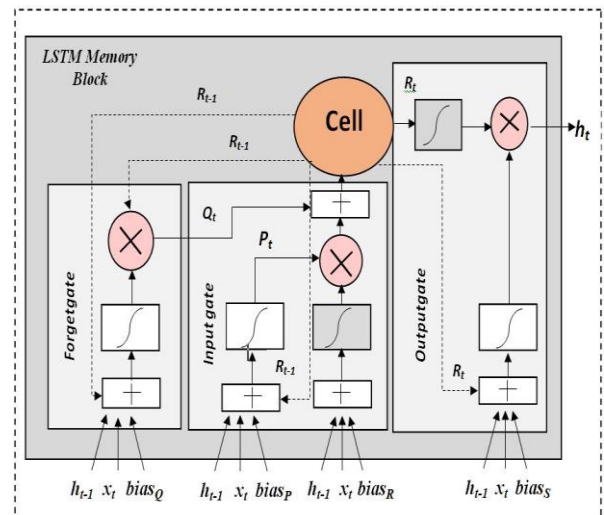


Fig. 4 Memory Block of LSTM

The LSTM equation can be expressed as follows:

$$P_t = \rho(\omega_{mp}x_t + \omega_{hp}h_{t-1} + \omega_{Rp}R_{t-1} + bias_p) \quad (19)$$

$$Q_t = \rho(\omega_{mQ}x_t + \omega_{hQ}h_{t-1} + \omega_{RQ}R_{t-1} + bias_Q) \quad (20)$$

$$R_t = Q_t R_{t-1} + P_t \tanh(\omega_{mR}x_t + \omega_{hR}h_{t-1} + bias_R) \quad (21)$$

$$S_t = \rho(\omega_{mS}x_t + \omega_{hS}h_{t-1} + \omega_{RS}R_t + bias_S) \quad (22)$$

$$h_t = S_t \tanh(R_t) \quad (23)$$

The only one-layer neural network in the memory block controlled the forget gate. P_t is the input gate, Q_t is the forget gate, S_t is the output gate, and R_t is the activation cell. The activation function of the forget gate is defined in equation (20). weight vector is represented ϖ for each input, and the bias represents the bias vector. ρ Represents the logistic sigmoid function and input features is represented by x_t . Previous block memory is represented by R_{t-1} , and the output of the previous block is represented by the h_{t-1} . The output of the forget gate multiplies with the memory block of the previous block. As a result, the effectiveness of the previous block on the current LSTM is determined. Suppose the value of the output vector is near zero, then it will erase the previous memory. The memory in the input gate and other gates is created by the simple neural network and the tanh activation function. The equation of the LSTM model has been defined above. The output of the LSTM block is calculated by equation (23).

The BiLSTM model removes various problems that were present in the previous RNN model. The BiLSTM model is the combination of two LSTM networks. It contains two passes; the forward pass and the backward pass. The forward and backward passes are the same, but the only difference is in the weight update method. In the forward pass, the weight is updated in a forward direction, and in the backward pass, the weight is updated in the backward direction. The same input sequence is given to both the passes, and the output connects to the same output layer to generate the output information. The equation of the bidirectional LSTM is given below:

$$l_t^1 = H(\varpi_{ml^1} x_t + \varpi_{l^1} l_{t-1}^1 + bias_{l^1}) \quad (24)$$

$$l_t^2 = H(\varpi_{ml^2} x_t + \varpi_{l^2} l_{t-1}^2 + bias_{l^2}) \quad (25)$$

$$y_t = \varpi_{l^1 y} l_t^1 + \varpi_{l^2 y} l_t^2 + bias_y \quad (26)$$

The equation to update the output is mentioned above. The world cup optimization technique is used to update the weights on the LSTM receiving signal.

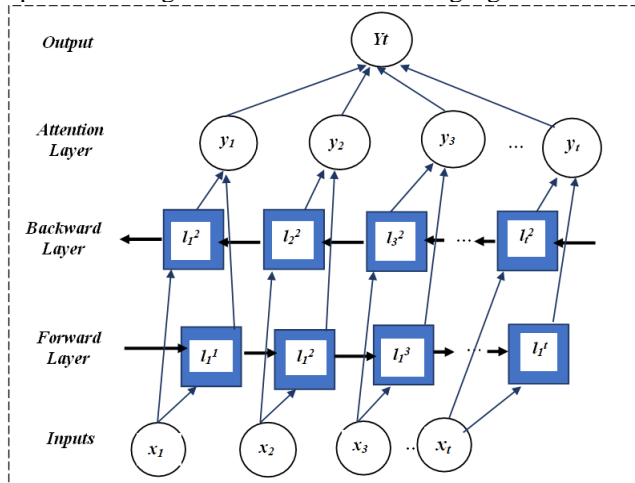


Fig. 5 BiLSTM trained by WCO

Fig. 5 depicts the layers of the BiLSTM as well as the weight update. The output of the BiLSTM is given to the input of the attention layer. The equation at the attention layer can be denoted as:

$$Y_t = l_t^1 \oplus l_t^2 \quad (27)$$

Feature vectors that the BiLSTM generates are read by the translator and reduced into the fixed-length vectors causing data loss. At this point, the attention layer allows the machine translator to examine the feature vectors. The output of the BiLSTM is compared with the ground truth value of the image at the attention layer. In the proposed work, a single attention layer mechanism was used that was broad enough to extract ridge features. At the attention layer, t^{th} feature-based input is represented by the above equation. Let y be a matrix made up of the LSTM layer's output vectors $[y_1, y_2, \dots, y_t]$.

The representation of the image denoted by α that is defined below:

$$\eta = \tanh(y) \quad (28)$$

$$\lambda = \text{soft max}(\alpha^T \eta) \quad (29)$$

$$\alpha = y \lambda^t \quad (30)$$

Where α^T is the transpose of the trained parameter, and α is the trained parameter that focuses on the fingerprint image's ridge and valley? S^α, t and S^α are the dimension of the α, λ and η . The softmax classifier was used in the output, classifying the latent fingerprint image into fingerprint and non-fingerprint regions.

C. World Cup optimization Algorithm

In the proposed work, the WCO algorithm is used for the weight update. The gradient-based back-propagation is the local search algorithm, while the WCO is the global search algorithm. This algorithm is based on the FIFA world cup and minimizes the root mean square of the neural network. The performance of the segmentation is directly dependent on the training of the LSTM model. The main goal of the WCO algorithm is to minimize the mean square error (MSE) at training time. Teams participating in FIFA are classified into seeds according to their rank. All the strong teams have been placed into one seed, and the weaker team placed into another seed. Initially, not all strong teams compete with each other. The teams in the WCO algorithm are organized into a group of clusters, and this group of clusters as continents. The algorithm of WCO can be defined as follow:

- 1) a) The first step is to initialize the continents and the team

Suppose there are C continents in the P variable dimension ($Pvar$) optimization problem. A continent is an array of $1 * Pvar$ dimensions, and it depicts the continent's current competing teams in the competitions. The following is the definition of this array:

$$Continent = [country_1, country_2, \dots, country_{Pvar}] \quad (31)$$

$$\text{Country}_j = [z_1, z_2, z_3, \dots, z_{Pvar}] \quad (32)$$

Here the variables ($z_1, z_2, z_3, \dots, z_{Pvar}$) are the floating-point numbers, and the z_j represents the j th team of the country. With the help of the rank function (f_r), the rank of each continent can be calculated.

$$\text{Rank} = f_r(z_1, z_2, z_3, \dots, z_{Ovar}) \quad (33)$$

$$O = C * P \quad (34)$$

Where C is the number of continents and P is the dimension of the variable.

b) Evaluation of the fitness function

The continent score is computed in the second stage. The WCO [29] algorithm computes the continent score by calculating the mean value and standard deviation for each continent as follows:

$$\bar{Z} = \frac{1}{n} \sum_{j=1}^n Z_j \quad (35)$$

$$SD = \sqrt{\frac{1}{n} \sum_{\kappa=1}^n Z_j - \bar{Z}} \quad (36)$$

Where n is the number of members in continent Z, SD is the Standard Deviation of continent Z, and the mean value of continent Z is \bar{Z} .

c) The continent rank is calculated as follows

$$\text{rank} = \frac{(\alpha \times SD + \bar{Z})}{2} \quad (37)$$

Where α is the coefficient used to decrease or increase the SD, and the range of α lies between [0, 1].

d) Team Rank

The teams are ranked as follows (according to their rank, all the continents are sorted, by default considering 5 continents and n teams):

$$Z_1 = [Z_{11}, \dots, Z_{1n}]^T \quad (38)$$

$$Z_2 = [Z_{21}, \dots, Z_{2n}]^T \quad (39)$$

$$Z_3 = [Z_{31}, \dots, Z_{3n}]^T \quad (40)$$

$$Z_4 = [Z_{41}, \dots, Z_{4n}]^T \quad (41)$$

$$Z_5 = [Z_{51}, \dots, Z_{5n}]^T \quad (42)$$

$$Z_{total} = [Z_{11}, \dots, Z_{1n}, Z_{21}, \dots, Z_{2n}, Z_{31}, \dots, Z_{3n}, Z_{41}, \dots, Z_{4n}, Z_{51}, \dots, Z_{5n}]^T \quad (43)$$

The weights for the solution are sorted in this phase. The continents with the lowest rank are chosen as the best solution. The goal of fitness is to find the lowest rank. The best solution is the minimum of Z_{total} .

$$Z_{Top} = \min(Z_{total}) \quad (44)$$

e) Start the competition at the next level

This section differs from real FIFA competitions because it is heuristic. The two-part vector can be used for this process in the following manner:

$$\text{pop} = Z_{total} = [Z_{best}, Z_{rand}] \quad (45)$$

Where Z_{rand} is the random value, and the Z_{best} is a vector as follow:

$$U_B = \frac{1}{2} \times ac \times (UB + LB) \quad (46)$$

$$L_B = \frac{1}{2} \times ac \times (UB - LB) \quad (47)$$

UB and LB are the problem's upper and lower bounds, respectively, and ac is the accuracy coefficient between the lower and upper bound.

f) Exploration and Exploitation

The Xrand and the Xbest can define the exploration and exploitation part of the algorithm. Xrand is the random value in the search space, and Xbest is the team's best score in the competition. The cross point (CP) separates the Xbest and Xrand, given by the following equation.

$$Z_{rand} = \text{pop}(1:CP, C) \quad (48)$$

$$Z_{best} = \text{pop}(CP+1:C, P) \quad (49)$$

The size of the new population is $M * N$. After generating a new population, the size is divided into m team and n continents.

$$\text{pop} = [Z_{best}, Z_{rand}] \begin{cases} Z_{1new}[pop(1:p)] \\ Z_{2new}[pop(p+1:q)] \\ Z_{3new}[pop(q+1:r)] \\ Z_{gnew}[pop(r+1:s)] \end{cases} \quad (50)$$

The WCO algorithm is used to update the weight of BiLSTM with two hidden layers. The main two aspects of the process are candidate representation and fitness selection. The system's vectors are a collection of weights joining the input layer and the hidden layer (l^1, l^2), a set of biased connecting in the hidden layer, and weights connecting with the hidden layer and the output layer. The length of the vector equals the number of weights and biases in the network, which may be determined as follows:

$$\text{len} = (\text{input}_{var} \times 2 \cdot ne) + (4 \times ne) + 1 \quad (51)$$

Where ne is the neurons in the hidden layer, and var is the input variable. The value 2 in the first term represents the double hidden layer in the network. The mean square error is used as a fitness function to measure the value generated by the continents, with the actual and predicted values employed in the calculation.

$$MSE = \frac{1}{n} \sum_{j=1}^n \left(Z_j - \hat{Z}_j \right)^2 \quad (52)$$

Where Z_j is the predicted value, and \hat{Z}_j is the estimated value? The population is then updated and iterated for the maximum number of iterations.

V. RESULTS AND DISCUSSION

All simulations are performed in the PYTHON Platform. IIIT-D database contains latent fingerprints impressions of all 10 fingers of 15 subjects. These fingerprints were extracted from two different surfaces tile and cards. A total of 1046 fingerprints are available in the IIIT-D dataset. The 32*32 size patches were used to train and test the neural network.

Fig. 6 shows the patches of fingerprint and non-fingerprint. The patches of fingerprint and non-fingerprint are used in the training of neural networks

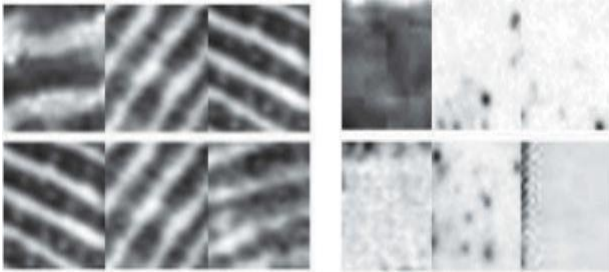


Fig. 6 (a) Fingerprint Blocks, (b) Non-Fingerprint Blocks

The output of BiLSTM is compared with the ground truth at the attention layer to generate the segmented image. WCO algorithm is used to train the BiLSTM, and it provides the optimal global solution; here, the probability of incorrect segmentation becomes low.

The algorithm was evaluated on the IIIT-D dataset. Table 1 displays the algorithm's output. The proposed model has been compared with various algorithms which are used for latent fingerprint segmentation. Correctly classified images calculate the accuracy of the latent fingerprint. The true positive rate (also known as sensitivity) of a fingerprint image can be computed as:

$$T_{pr} = \frac{T_p}{T_p + F_n} \quad (53)$$

Where T_p is truly positive, and F_n is a false negative.

The true negative rate can be calculated (Also called specificity) as:

$$T_{nr} = \frac{T_n}{T_n + F_p} \quad (54)$$

Where T_n is a true negative, and F_p is a false positive.

False detection rate (FDR) gives the wrong prediction on non-fingerprint images as fingerprint images. It can be calculated as:

$$FDR = \frac{F_p}{T_n + F_p} \quad (55)$$

Miss Detection Rate (MDR) gives the wrong prediction on fingerprint images classified into non-fingerprint images. It can be calculated as:

$$MDR = \frac{F_n}{T_p + F_n} \quad (56)$$

Fig. 7 shows the results of the proposed algorithm. Fig 7(a) represents the raw image taken from the IIITD data set, and Fig 7(b) represents the segmented images. The proposed model obtains high segmentation accuracy as compared to the previous algorithms. MDR is 9.7%, and the FDR is 4.13% in the proposed algorithm. The proposed algorithm was compared with the existing algorithm for latent fingerprint segmentation. Table 1 provides a summarized comparison study of these strategies. The comparison shows that the proposed method gave better results than the previous methods of latent fingerprint segmentation

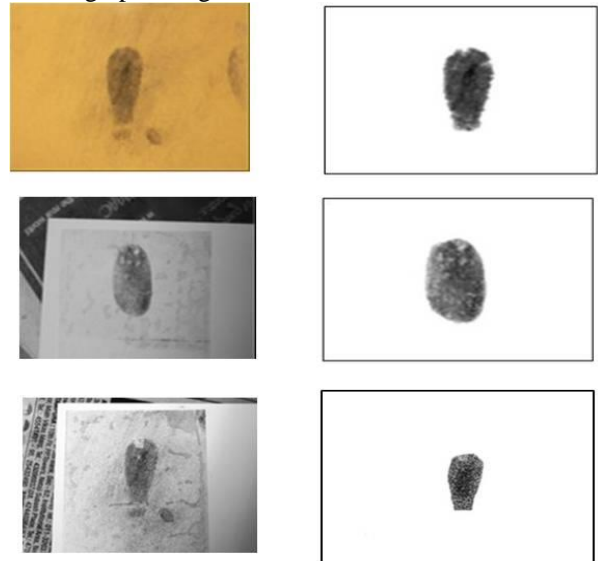


Fig.7 a) Raw (Original) Image, b) Segmented image

Table-1: Comparison of performance of different segmentation techniques.

Segmentation Approaches	Database	MDR	FDR
ATV[09]	NIST SD27	14.10%,	26.13%
ADTV[11]	NIST SD27	14.10%	26.1%
Fractal Dimension [12]	NIST SD27	9.22%	18.7%
	WVU DB	15.54%,	9.65%
	IIITD	6.38%	10.07%
Ridge orientation and frequency computation[13]	NIST SD27	14.78%	47.99%
Patched Based[28]	IIITD	13.80%	5.2%
Proposed Algorithm	IIITD	9.7%	4.13%

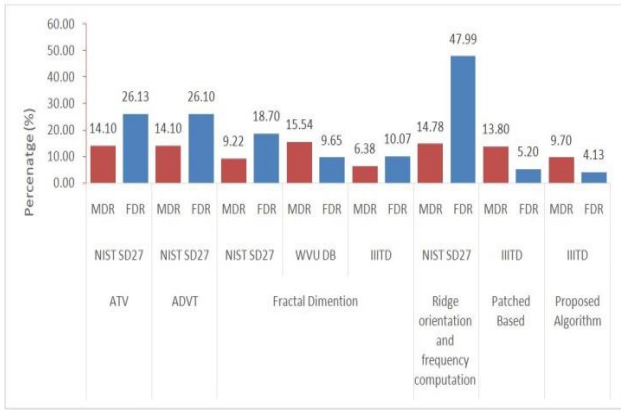


Fig. 8 Segmentation Reliability in several datasets

Fig. 8 shows the comparison of the proposed algorithm with the previously developed algorithms for the latent fingerprint segmentation. The result shows proposed algorithm produces better segmentation than the previous algorithms. The MDR and FDR are lesser in the output generated by the proposed algorithm that increases the segmentation accuracy. III-D data set has been used as it is publically available.

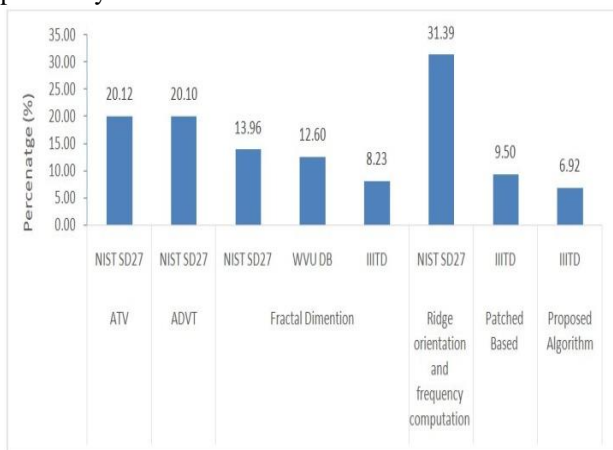


Fig. 9 Average Segmentation Reliability in several datasets

Fig. 9 shows the average of the MDR and FDR. The result shows the average value is 6.92% in the proposed work, which is better than the results generated from the previous algorithms on latent fingerprint segmentation.

VI. CONCLUSION

Fingerprints have been of great interest and help for the forensic department for the identification of criminals. The matching accuracy of plain/rolled fingerprints has been good due to the fine quality, but different types of noises present in latent fingerprints lead to low matching accuracy and remain a challenging area. Latent Fingerprints require manual interventions for fingerprint feature extraction and matching them with the reference database and suspects' fingerprints. The matching accuracy of Latent fingerprints depends on segmentation accuracy and quality. Segmentation separates the fingerprint and non-fingerprint area using algorithms. Existing segmentation algorithms pose a challenge because

they don't perform well on latent fingerprints since they have high FDR and MDR.

This research proposes a new algorithm for latent fingerprint segmentation that overcomes the problems present in the manual and semiautomatic segmentation approaches. The proposed work reduces the MDR and FDR to increase the segmentation accuracy. Gradient, frequency, and ridge methods were used for the feature extraction of the latent fingerprints. These features were used in the training of neural networks in BiLSTM. The WCO algorithm is used to train and test the neural network for segmentation. WCO assists neural networks in determining the ideal initial weights, decreasing MSE error, and increasing convergence speed. The proposed algorithm was also compared with the previous segmentation algorithms, and it has obtained 92.9% accuracy.

The latent fingerprint dataset of the IIIT-D database was used to test the proposed algorithm.

REFERENCES

- [1] Champod, C. Lennard, P. Margot, and M. Stoilovic, Fingerprints and Other Ridge Skin Impressions. CRC Press, (2004).
- [2] S. A. Cole, Suspect Identities: A History of Fingerprinting and Criminal Identification. Harvard University Press, (2002).
- [3] Jain, A. K., & Feng, J., Latent fingerprint matching. IEEE Transactions on pattern analysis and machine intelligence.33 (1) (2010) 88-100.222
- [4] Mehtre, B. M., Murthy, N. N., Kapoor, S., & Chatterjee, B., Segmentation of fingerprint images using the directional image. Pattern recognition.20(4) (1987) 429-435.
- [5] Mehtre, B. M., & Chatterjee, B., Segmentation of fingerprint images—a composite method. Pattern recognition, 22(4) (1989) 381-38
- [6] Ratha, N. K., Chen, S., & Jain, A. K., Adaptive flow orientation-based feature extraction in fingerprint images. Pattern Recognition, 28(11) (1995) 1657-1672.
- [7] Bazen, A. M., & Gerez, S. H., Segmentation of fingerprint images. In ProRISC 2001 Workshop on Circuits, Systems and Signal Processing (2001)276-280.
- [8] Xue, J., & Li, H., Fingerprint image segmentation based on a combined method. In 2012 IEEE International Conference on Virtual Environments Human-Computer Interfaces and Measurement Systems (VECIMS) Proceedings IEEE. (2012) 207-208
- [9] Zhang, J., Lai, R., & Kuo, C. C. J., Latent fingerprint segmentation with adaptive total variation model. In 2012 5th IAPR International Conference on Biometrics (ICB) IEEE. (2012)189-195
- [10] Zhang, J., Lai, R., & Kuo, C. C. J. (2012, September). Latent fingerprint detection and segmentation with a directional total variation model. In 2012 19th IEEE International Conference on Image Processing IEEE.(2012)1145-1148
- [11] Zhang, J., Lai, R., & Kuo, C. C. J., Adaptive directional total-variation model for latent fingerprint segmentation. IEEE Transactions on Information Forensics and Security. 8(8)(2013)1261-1273.
- [12] Choi, H., Boaventura, M., Boaventura, I. A., & Jain, A. K., Automatic segmentation of latent fingerprints. In 2012 IEEE Fifth International Conference on Biometrics: Theory, Applications and Systems (BTAS) IEEE.(2012)303-310
- [13] Short, N. J., Hsiao, M. S., Abbott, A. L., & Fox, E. A., Latent fingerprint segmentation using ridge template correlation. In 4th International Conference on Imaging for Crime Detection and Prevention IET.(2011)1-6
- [14] Cao, K., Liu, E., & Jain, A. K., Segmentation and enhancement of latent fingerprints: A coarse to fine ridge structure dictionary. IEEE transactions on pattern analysis and machine intelligence.36(9)(2014)1847-1859.
- [15] Sankaran, A., Jain, A., Vashisth, T., Vatsa, M., & Singh, R. (2017). Adaptive latent fingerprint segmentation using feature selection and

- random decision forest classification. *Information Fusion*.34 (2017) 1-15.
- [16] Stojanović, B., & Marques, O., Machine Learning Based Overlapped Latent Fingerprints Segmentation and Separation. In 2018 26th Telecommunications Forum (TELFOR)IEEE.(2018)1-8
- [17] Jain, A. K., & Feng, J., Latent fingerprint matching. *IEEE Transactions on pattern analysis and machine intelligence*, 33(1) (2010) 88-100.
- [18] Bazen, A. M., & Gerez, S. H. Segmentation of fingerprint images. In *ProRISC 2001 Workshop on Circuits, Systems and Signal Processing*, Veldhoven, The Netherlands.(2001) 276-280.
- [19] Maltoni, D., Maio, D., Jain, A. K., & Prabhakar, S., *Handbook of fingerprint recognition*. Springer Science & Business Media. (2009)
- [20] NIST, NFIQ 2.0, Quality features definition, http://biometrics.nist.gov/cs_links/quality/NFIQ_2/NFIQ-2_Quality_Feature_Defin-Ver05.pdf.
- [21] E. Zhu, J. Yin, C. Hu, G. Zhang, A systematic method for fingerprint ridge orientation estimation and image segmentation, *Pattern Recognition*.39(8)(2006)1452–1472.
- [22] Chen, X., Tian, J., Cheng, J., & Yang, X., Segmentation of fingerprint images using a linear classifier. *EURASIP Journal on Advances in Signal Processing*.2(4)(2004)1-15.
- [23] Chikkerur, S., Govindaraju, V., & Cartwright, A. N., Fingerprint image enhancement using STFT analysis. In *International Conference on Pattern Recognition and Image Analysis* Springer, Berlin, Heidelberg. (2005) 20-29.
- [24] Chin, Y. J., Ong, T. S., Teoh, A. B. J., & Goh, K. O. M., Integrated biometrics template protection technique based on fingerprint and palmprint feature-level fusion. *Information Fusion*.18 (2014) 161-174.
- [25] Elfaik, H. Deep Bidirectional LSTM Network Learning-Based Sentiment Analysis for Arabic Text. *Journal of Intelligent Systems*. 30(1)(2021) 395-412.
- [26] Liu, Q., Zhou, F., Hang, R., & Yuan, X, Bidirectional-convolutional LSTM based spectral-spatial feature learning for hyperspectral image classification. *Remote Sensing*. 9(12)(2017)1330.
- [27] Chaudhary, N., Singh, H. P., & Dimri, P., Comparative Study of Latent Fingerprint Image Segmentation Techniques Based on Literature Review. *Ambient Communications and Computer Systems*. (2020) 391-399.
- [28] Khan, A. I., & Wani, M. A., Patch-based segmentation of latent fingerprint images using convolutional neural network. *Applied Artificial Intelligence*. 33(1) (2019) 87-100.
- [29] Razmjoooy, N., Estrela, V. V., & Loschi, H. J, Entropy-based breast cancer detection in digital mammograms using world cup optimization algorithm. *International Journal of Swarm Intelligence Research (IJSIR)*.11(3)(2020) 1-18.
- [30] Chaudhary, N., & Dimri, P., Singh, H. P., Segmentation of Latent Fingerprint using Neural Network. *International Journal of Engineering and Advanced Technology*. 9(1)(2019)3777-3780.
- [31] Yildirim, Ö. A novel wavelet sequence based on a deep bidirectional LSTM network model for ECG signal classification. *Computers in biology and medicine*.96 (2018) 189-202.